

DY Pegasi – a SX Phoenicis Star in a Binary System with an Evolved Companion

HUI-FANG XUE¹ AND JIA-SHU NIU^{2,3,4}

¹*Department of Physics, Taiyuan Normal University, Taiyuan, 030619, China*

²*Institute of Theoretical Physics, Shanxi University, Taiyuan 030006, China*

³*State Key Laboratory of Quantum Optics and Quantum Optics Devices, Shanxi University, Taiyuan 030006, China*

⁴*Collaborative Innovation Center of Extreme Optics, Shanxi University, Taiyuan, Shanxi 030006, China*

ABSTRACT

In this work, the photometric data from AAVSO are collected and analyzed on the SX Phoenicis star DY Pegasi (DY Peg). From the frequency analysis, we get 3 independent frequencies: $f_0 = 13.71249 \text{ c days}^{-1}$, $f_1 = 17.7000 \text{ c days}^{-1}$, and $f_2 = 18.138 \text{ c days}^{-1}$, in which f_0 and f_1 are the radial fundamental and first overtone mode respectively, while f_2 is detected for the first time and should belong to a non-radial mode. The $O-C$ diagram of the times of maximum light shows that DY Peg has a period change rate $(1/P_0)(dP_0/dt) = -(5.87 \pm 0.03) \times 10^{-8} \text{ yr}^{-1}$ for its fundamental pulsation mode, and should belong to a binary system which has a orbital period $P_{\text{orb}} = 15425.0 \pm 205.7 \text{ days}$. Based on the spectroscopic information, single star evolutionary models are constructed to fit the observed frequencies. However, some important parameters of the fitted models are not consistent with that from observations. Combing with the information from observation and theoretical calculation, we conclude that DY Peg should be a SX Phoenicis star in a binary system and accreting mass from a dust disk, which is the residue of its evolved companion (most probability a white dwarf at the present stage) in the AGB phase. Further observations are needed to confirm this inference, and it might be potentially a universal formation mechanism and evolutionary history for SX Phoenicis stars.

1. INTRODUCTION

SX Phoenicis (SX Phe) stars, a subgroup of the high-amplitude δ Scuti stars (HADS), are old Pop. II stars. They always pulsate in single or double radial modes (such as SW Ser, AE UMa, etc.), but some also show non-radial modes coupling with the radial modes. Because of the insufficient amount and the generally poor photometric precision of the observation data, whether any low-amplitude pulsations exist besides the dominant radial modes in most SX Phe stars are still unknown. Although most SX Phe stars, which are characterized by high amplitudes of pulsation, low metallicity, and large spatial motion, are found to be members of globular clusters (Rodríguez & López-González 2000), some of them have been discovered in the general star fields (Rodríguez & Breger 2001). Particularly, pulsations in the majority of the field SX Phe variables display very simple frequency spectra with short periods ($\leq 0^{\text{d}}.08$) and large visual peak-to-peak amplitudes ($\geq 0^{\text{m}}.1$, c.f. (Fu et al. 2008)). There are several scenarios

proposed to illustrate the formation mechanism and evolutionary history of SX Phe stars (see, e.g., Rodríguez & López-González (2000)), but the origin of them is still unknown up to now.

DY Peg is a SX Phe star with a low metallicity ($[\text{Fe}/\text{H}] = -0.8$, Burki & Meylan (1986) and Hintz et al. (2004); $[\text{Fe}/\text{H}] = -0.56$, Peña et al. (1999)). The variability of DY Peg was discovered by Morgenroth (1934). Whereafter a number of photometric monitoring were taken to record and analyze its behavior of lightness variation, such as Iriarte (1952); Meylan et al. (1986); Percy et al. (2007), etc. Based on the secular observations, the period change of DY Peg was continuously determined by Quigley & Africano (1979); Mahdy & Szeidl (1980); Pena & Peniche (1986); Derekas et al. (2003); Hintz et al. (2004); Derekas et al. (2009); Fu et al. (2009). Li & Qian (2010) did a more detailed research on the period change of this star, in which they reported the variation of the period can be described by a secular decrease of the period at a rate of $-6.59 \times 10^{-13} \text{ days cycle}^{-1}$, and a perturbation from a companion star in an eccentric orbit with a period of 15414.5 days. Unlike the period change which has been studied adequately, the pulsation frequency of DY Peg was not detected accurately besides the fundamental mode. Garrido & Rodriguez (1996)

Corresponding author: Jia-Shu Niu
 jsniu@sxu.edu.cn

and Pop et al. (2003) reported that DY Peg should be a double-mode pulsator, while it was not confirmed in subsequent works (Fu et al. 2009; Barcza & Benkő 2014).

In the following sections, we extract some important information from observations, construct theoretical models and present some discrepancies between observation and theoretical calculation. Then, we propose some inferences to relieve the discrepancies and backtrack the evolutionary history of DY Peg. This paper is organized as follows: Section 2 presents the data reduction procedures from observations; theoretical models are constructed and the calculation results are shown in Section 3; Section 4 gives the discussion and conclusions.

2. OBSERVATIONS AND ANALYSIS

2.1. Observations

The time-series photometric data in V band on DY Peg is downloaded from the American Association of Variable Star Observers (AAVSO) International Database (Kafka 2020), which cover from 2003 August to 2019 December. After the heliocentric corrections of the Julian date and magnitude shifts elimination between different nights, the light curves are used to extract the times of maximum light (see in Appendix, Figure 3). A portion of the light curves covering a period of 32 days (from 2011 October 30 to 2011 December 1) are used to make frequency analysis. Table 3 in Appendix lists the detailed information of the observations for the frequency analysis, and Figure 4 in Appendix shows the relevant light curves.

2.2. Frequency Analysis

The software Period04 (Lenz & Breger 2005) is used to perform Fourier transformations and frequency pre-whitening process for the light curves of DY Peg. Figure 5 in Appendix shows the spectral window and Fourier amplitude spectra of the pre-whitening process. The statistical criterion of an amplitude signal-to-noise ratio is set to be 4.0 for judging the reality of a newly discovered peak in the Fourier spectra (Breger et al. 1993). The noises are determined as the mean amplitudes around each peak with a box of 6 $c\text{ days}^{-1}$.

In total, 14 statistically significant frequencies have been detected, including 3 independent frequencies ($f_0 = 13.71249 \text{ c days}^{-1}$, $f_1 = 17.7000 \text{ c days}^{-1}$, and $f_2 = 18.138 \text{ c days}^{-1}$) and 11 harmonics or linear combinations of them. The solid curves in Figure 4 in Appendix show the fits with the multi-frequency solution which are listed in Table 1.

The first pulsation mode with frequency $f_0 = 13.71249 \text{ c days}^{-1}$ and amplitude $a_0 = 240.3 \text{ mmag}$ dominates the light curves of DY Peg. The secondary

pulsation mode with frequency $f_1 = 17.7000 \text{ c days}^{-1}$ and a small amplitude $a_1 = 5.2 \text{ mmag}$ is obvious in present work, which was not confirmed in previous works because of the low signal-to-noise (see Garrido & Rodriguez (1996), Pop et al. (2003), Fu et al. (2009), and Barcza & Benkő (2014)).

The ratio of $f_0/f_1 = 0.775$ agrees well with the theoretical calculation on the fundamental and first overtone radial modes (~ 0.77 , see Petersen & Christensen-Dalsgaard (1996); Poretti et al. (2005)), illustrating DY Peg does pulsate in the two radial modes.

What is interesting is that a third independent frequency solution with frequency $f_2 = 18.138 \text{ c days}^{-1}$ and amplitude $a_2 = 2.8 \text{ mmag}$ is detected for the first time in this work. f_2 is close to f_1 with a smaller amplitude, therefore, we suggest that f_2 should be a non-radial mode.¹ For a definite mode identification of f_2 , multicolour photometry or time resolved high resolution spectroscopy is needed.

2.3. The $O - C$ Diagram²

Based on the observations between 2003 and 2019 (see Figure 3 in Appendix), the light curves around the maxima were fitted by a fourth polynomial. We have obtained 139 times of maximum light from these light curves, and estimated their uncertainties via Monte Carlo simulations. The newly determined times of maximum light and the uncertainties are listed in Table 4 in Appendix. In Li & Qian (2010), 412 pe/CCD times of light maximum of DY Peg have been collected, which are also used in our $O - C$ analysis. In addition, 138 times of maximum light in V band are collected from the literature, which are listed in Table 5 in Appendix. Totally, 689 times of maximum light spanning 70 years are used to perform the $O - C$ analysis in this work.³

As that have been shown in Li & Qian (2010), a linear or quadratic fit cannot reproduce the times of light maximum precisely. Consequently, we fit the times of light maximum with a quadratic plus a function of sines, which imply they are affected by the linear change of the pulsation period of the star and by a light traveling time effect of the star in a binary system of an elliptical orbit (Paparo et al. 1998). The calculated times of light

¹ The ratio of $f_0/f_2 = 0.756$ can rule out the assumption that f_2 is a radial mode.

² Because the amplitude of f_0 is about 46 times larger than that of f_1 and the times of maximum light are dominated by the f_0 mode, $O - C$ method can be used effectively to analyze the pulsating and orbital parameters in this case.

³ In the following analysis, we give typical uncertainties 0.0006 days and 0.0005 days to the times of maximum light in the literature detected by photoelectric photometers and CCD cameras respectively, which did not give corresponding uncertainties.

Table 1. Multi-frequency solution of the light curves of DY Peg in 2011. Note: σ_f denotes the error estimation of frequency, σ_a denotes the error estimation of amplitude. All of them are calculated based on the formulas given by Montgomery & Odonoghue (1999).

NO.	Marks	Frequency (c days $^{-1}$)	σ_f (c days $^{-1}$)	Amplitude (mmag)	σ_a (mmag)	S/N
F1	f_0	13.71249	0.00001	240.3	0.2	112.6
F2	$2f_0$	27.42506	0.00004	82.2	0.2	104.2
F3	$3f_0$	41.1374	0.0001	28.3	0.2	68.8
F4	$4f_0$	54.8502	0.0003	12.1	0.2	45.2
F5	f_1	17.7000	0.0006	5.2	0.2	6.6
F6	$5f_0$	68.5626	0.0007	5.0	0.2	25.7
F7	$f_1 - f_0$	4.016	0.001	2.9	0.2	4.8
F8	$f_0 + f_1$	31.412	0.001	2.7	0.2	6.1
F9	$6f_0$	82.275	0.001	2.7	0.2	13.4
F10	f_2	18.138	0.001	2.8	0.2	6.7
F11	$7f_0$	95.987	0.002	1.8	0.2	16.4
F12	$2f_0 + f_1$	45.122	0.002	1.7	0.2	6.1
F13	$f_0 + f_2$	31.851	0.002	1.7	0.2	6.8
F14	$8f_0$	109.702	0.003	1.2	0.2	6.7

maximum have the form

$$C = \text{HJD}_0 + P_0 \times E + \frac{1}{2}\beta E^2 + A[\sqrt{1-e^2} \sin \phi \cos \omega + \cos \phi \sin \omega], \quad (1)$$

where ϕ is the solution of Kepler's equation

$$\phi - e \sin \phi = \frac{2\pi}{P_{\text{orb}}}(P_0 \times E - t_0). \quad (2)$$

In the above formulas, HJD_0 is the initial epoch, P_0 is the pulsation period, β is the linear change of pulsation period, $A = a_1 \sin i/c$ is the projected semi-major axis, e is the eccentricity, ϕ is the eccentric anomaly, ω is the longitude of the periastron passage in the plane of the orbit, P_{orb} is the orbital period of the binary system, t_0 is the time of passage through the periastron. More details of the light-time orbit equation can be found in Irwin (1952).

The Markov Chain Monte Carlo (MCMC) algorithm is used to determine the posterior probability distribution of the parameters in Eq. (1) and (2).⁴ The samples of the parameters are taken as their posterior probability distribution function (PDF) after the Markov Chains have reached their equilibrium states. The mean values and the standard deviation of the parameters are listed in Table 2, and the best-fit result (which gives $\chi^2/\text{d.o.f.} = 61.57$) of the $O - C$ values (excluding the linear part) and the corresponding residuals are shown

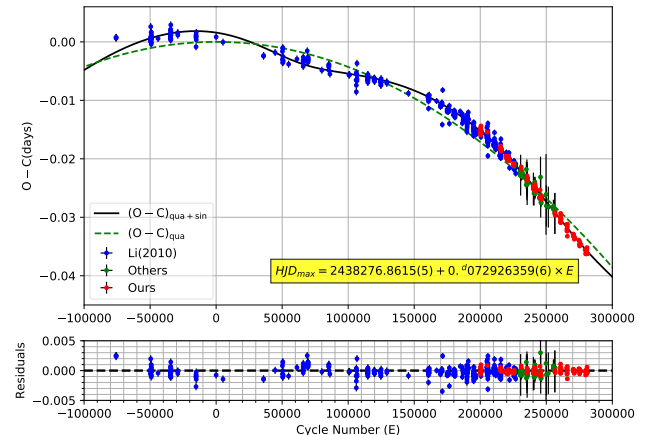


Figure 1. The $O - C$ values (excluding the linear part HJD_{max}) and the corresponding residuals. In the upper panel, the black line represents the best-fit result of a quadratic plus a light-time orbit equation, the green dashed line represents the quadratic part. In the lower panel, the residuals of the best-fit result are plotted. The data collected from Li & Qian (2010) are shown in blue points; the data from historical literature are shown in green points; the data from present work are shown in red points.

in Figure 1. Benefited from the additional times of maximum light, the errors of the parameters are obviously smaller than that in Li & Qian (2010) by a factor of 2 to 10, which provide us a highly credible result for the subsequent discussion.

⁴ The PYTHON module `emcee` (Foreman-Mackey et al. 2013) is employed to perform the MCMC sampling. Some examples can be found in Niu & Li (2018); Niu et al. (2018, 2019).

3. THEORETICAL MODELS

Table 2. The pulsating and orbital parameters of DY Peg. Note that the values of $a_1 \sin i$ and $(1/P_0)(dP_0/dt)$ are derived from the values of A and β respectively. The value of $f(M)$ (mass function) is derived from the values of $a_1 \sin i$ and P_{orb} .

Parameter	value
HJD ₀	2438276.86155 ± 0.00007
P_0 (days)	0.0729263596 ± 0.0000000006
β (day cycle ⁻¹)	$(-8.55 \pm 0.04) \times 10^{-13}$
A (days)	0.00204 ± 0.00003
e	0.244 ± 0.008
P_{orb} (days)	15425.0 ± 205.7
t_0	2457941.8 ± 158.7
ω	239.3 ± 5.2
$a_1 \sin i$ (AU)	0.353 ± 0.005
$(1/P_0)(dP_0/dt)$ (yr ⁻¹)	$-(5.87 \pm 0.03) \times 10^{-8}$
$f(M)$ (M_{\odot})	$(2.47 \pm 0.12) \times 10^{-5}$

Considering the orbital period $P_{\text{orb}} \sim 15400$ days, which is so large that DY Peg could not have a evolutionary history with severe mass transfer like that in the case of planetary nebulae (PNe) with binary central stars (see, e.g., Jones & Boffin (2017)), we attempt to determine its stellar mass and evolutionary stage based on the single star evolutionary models (see, e.g., Niu et al. (2017); Xue et al. (2018)).

The open source 1D stellar evolution code Modules for Experiments in Stellar Astrophysics (MESA; Paxton et al. 2011, 2013, 2015, 2018, 2019) is used to construct the structure and evolutionary models, together with the stellar oscillation code GYRE (Townsend & Teitler 2013) is used to compute the corresponding pulsation frequencies for a specific structure model.

The initial parameters which are used to construct pre-main sequence evolutionary models of DY Peg are configured as follows. Different metallicity [Fe/H] with the values of -1.0 , -0.8 , and -0.56 dex are considered as the initial metallicity of the evolutionary model (see Table 6 in Appendix for more details). According to the calculation based on the formulas listed in Appendix, we get 3 tuples ($X = 0.756$, $Z = 0.001$), ($X = 0.752$, $Z = 0.002$), and ($X = 0.744$, $Z = 0.004$), which are set as the initial inputs of the evolutionary models. The initial mass of the models are set in the interval from $0.8 M_{\odot}$ to $2.0 M_{\odot}$ with a step of $0.01 M_{\odot}$, covering the typical mass range of SX Phe stars (Mc-Namara 2011). In the model calculation, the rotation of the star has also been considered. Because Solano & Fernley (1997) provides us the projected rotational velocity $v \sin i = 23.6$ km s⁻¹, the equatorial rotation velocity $v_{\text{eq}} = 23.6$ km s⁻¹ and $v_{\text{eq}} = 150$ km s⁻¹ are set

to be the inputs in the model calculation, which covers a reasonable range of $\sin i$. The value of the mixing-length parameter is set to be $\alpha_{\text{MLT}} = 1.89$ (c.f. Breger (2000); Yang et al. (2012)). Every evolutionary track is calculated from zero-age main sequence to post-main sequence stage. The pulsation frequencies are calculated for every step in the evolutionary tracks. In the pulsation model calculation, f_0 and f_1 are considered to have the quantum numbers of ($l = 0$, $n = 1$) and ($l = 0$, $n = 2$), respectively.

Figure 2 shows the best-fit seismic models⁵ to the observed frequencies along with the evolutionary tracks for specific combinations of (Z , v_{eq}), in which the subfigure (a) is a Petersen diagram (the period ratio of the first overtone mode to the fundamental mode (P_1/P_0) as a function of the fundamental mode period (P_0)) and the subfigure (b) is a HertzsprungRussell diagram (H-R diagram).⁶ The non-radial modes are also calculated for these seismic models, and we find that f_2 with quantum numbers ($l = 1$, $n = 1$) can give us the best-fit to the observed value.

In the H-R diagram, it is clear that the best-fit seismic models (based on single star evolution models) to the observed pulsation frequencies cannot match the observed temperature and luminosity. What's more, these seismic models cannot match a period change of $(1/P_0)(dP_0/dt) = -(5.87 \pm 0.03) \times 10^{-8}$ yr⁻¹ either. Both of these discrepancies need additional interpretations.

4. DISCUSSION AND CONCLUSIONS

On one hand, the $O - C$ diagram provides us a clear evidence that the $O - C$ values could be well reproduced by a decrease of the pulsation period and a light traveling time effect of the star in a binary system of an elliptical orbit. On the other hand, the best-fit seismic models based on single star evolution show discrepancies with observed temperature and luminosity within uncertainties. All these results lead us to conclude that DY Peg should belong to a binary system.

Although we could not determine the mass of its companion because of the lacking information about the orbit inclination, we have some hints to infer the type of

⁵ More details can be found in Table 7 of Appendix.

⁶ The range of the observed effective temperature $T_{\text{eff}} \in [6750, 8350]$ K is taken from related literatures (see the detail in Table 6 in Appendix). The luminosity is calculated based on the distance, apparent magnitude, extinction, and bolometric correction. Considering the lightness variation of the star $\Delta V \sim 0.6$ mag, we finally get $\log L/L_{\odot} \in [1.07, 1.31]$. More details can be found in Appendix.

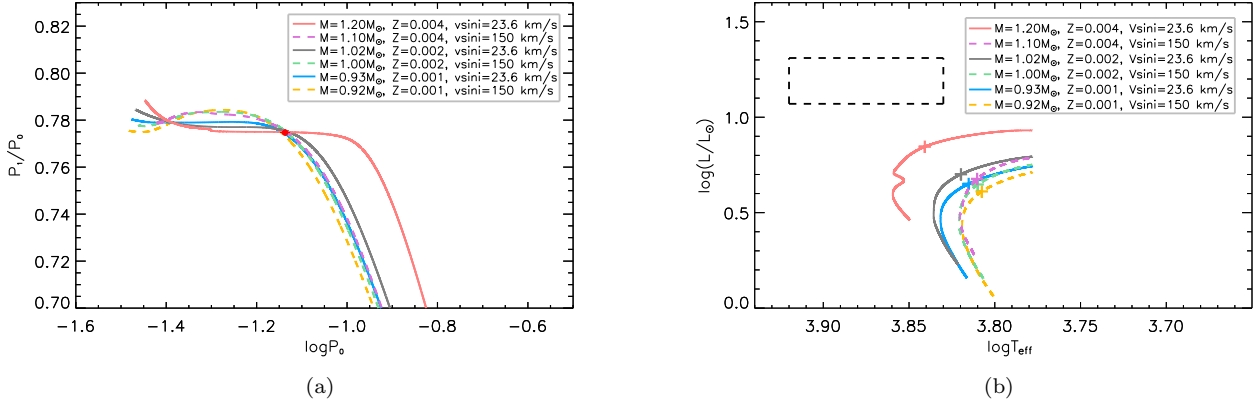


Figure 2. The 6 best seismic models for DY Peg along with the evolutionary tracks. In subfigure (a), the red point represents the observed value of P_1/P_0 and P_0 with uncertainties. In subfigure (b), the crosses on the evolutionary tracks represent the best seismic models; the region enclosed by dash lines represents the relevant uncertainties derived from observations.

the companion and then the evolution history of the binary system.

- (i) In the subfigure (b) of Figure 2, we can consider the dashed rectangle represents the temperature and luminosity of the binary system while the crosses represent the possible models of DY Peg.⁷ Consequently, if the companion has higher temperature (hotter) and remarkable luminosity (not that faintness), the discrepancy could hopefully be relieved. The candidate of such type star should be a white dwarf (WD) or a subdwarf B (sdB) star rather than a brown dwarf (Li & Qian 2010).
- (ii) According to the spectroscopic observations of DY Peg, Hintz et al. (2004) found a slight (0.15 dex) excess of the α -elements calcium and sulfur, and a more significant (0.5 dex) excess of carbon. Because these elements could only be produced in the phase of asymptotic giant branch (AGB) according to the s-process element enrichment, DY Peg's atmosphere should have been polluted by the companion who have already discarded its envelope and become a WD (sdB stars can not generate these elements in their evolutionary history (Han et al. 2002, 2003)).

Moreover, the decrease period change of the fundamental mode $(1/P_0)(dP_0/dt) = -(5.87 \pm 0.03) \times 10^{-8} \text{ yr}^{-1}$ cannot be explained as the stellar evolution effect. In view of the above inferences, we interpret it as the result of the mass accretion from a dust disk around

⁷ Here, we insist that there have not been a severe mass transfer process in the evolution history of DY Peg, whose orbital period can reach up to ~ 15400 days. Consequently, the best-fit seismic models based on single star evolution could also represent the properties of DY Peg.

DY Peg, which is produced during the mass discarding of its companion in the AGB phase. In such case, the mass accretion rate of DY Peg should be in the range of $[1.18 \times 10^{-7}, 1.19 \times 10^{-7}] M_\odot \text{ yr}^{-1}$.⁸

In summary, in this work, we have (i) detected and confirmed $f_2 = 18.138 \text{ c days}^{-1}$ as a non-radial pulsation mode with quantum numbers ($l = 1, n = 1$) for the first time; (ii) confirmed DY Peg belongs to a binary system with a orbital period $P_{\text{orb}} = 15425.0 \pm 205.7$ days; (iii) confirmed the period change rate of fundamental mode of DY Peg $(1/P_0)(dP_0/dt) = -(5.87 \pm 0.03) \times 10^{-8} \text{ yr}^{-1}$; (iv) combined the information from observation and theoretical calculation, inferred that DY Peg should be accreting mass from a dust disk, which is the residue of its evolved companion (most probability a WD at the present stage) in the AGB phase. In order to confirm the inferences, more precise spectroscopic and photometric observations are needed. Whether every SX Phe star has a evolutionary history in a binary system, whose companion evolved faster than it and transferred mass to it, should be tested and verified in the future.

ACKNOWLEDGMENTS

We acknowledge with thanks the variable star observations from the AAVSO International Database contributed by observers worldwide and used in this research. This research was supported by the Special Funds for Theoretical Physics in National Natural Science Foundation of China (NSFC) (No. 11947125) and the Applied Basic Research Programs of Natural Science Foundation of Shanxi Province (No. 201901D111043).

⁸ This value can be calculated by the periodluminositycolour relation (Breger & Pamyatnykh 1998).

Facility: AAVSO

Software: emcee (Foreman-Mackey et al. 2013), Period04 (Lenz & Breger 2005), MESA (Paxton et al. 2011, 2013, 2015, 2018, 2019), GYRE (Townsend & Teitler 2013)

REFERENCES

- Asplund, M., Grevesse, N., Sauval, A. J., & Scott, P. 2009, *ARA&A*, 47, 481, doi: [10.1146/annurev.astro.46.060407.145222](https://doi.org/10.1146/annurev.astro.46.060407.145222)
- Bailer-Jones, C. A. L., Rybizki, J., Fouesneau, M., Mantelet, G., & Andrae, R. 2018, *AJ*, 156, 58, doi: [10.3847/1538-3881/aacb21](https://doi.org/10.3847/1538-3881/aacb21)
- Barcza, S., & Benkő, J. M. 2014, *MNRAS*, 442, 1863, doi: [10.1093/mnras/stu978](https://doi.org/10.1093/mnras/stu978)
- Breger, M. 2000, in Astronomical Society of the Pacific Conference Series, Vol. 210, Delta Scuti and Related Stars, ed. M. Breger & M. Montgomery, 3
- Breger, M., & Pamyatnykh, A. A. 1998, *A&A*, 332, 958
- Breger, M., Stich, J., Garrido, R., et al. 1993, *A&A*, 271, 482
- Burki, G., & Meylan, G. 1986, *A&A*, 159, 261
- Derekas, A., Kiss, L. L., Székely, P., et al. 2003, *A&A*, 402, 733, doi: [10.1051/0004-6361:20030291](https://doi.org/10.1051/0004-6361:20030291)
- Derekas, A., Kiss, L. L., Bedding, T. R., et al. 2009, *MNRAS*, 394, 995, doi: [10.1111/j.1365-2966.2008.14381.x](https://doi.org/10.1111/j.1365-2966.2008.14381.x)
- Foreman-Mackey, D., Hogg, D. W., Lang, D., & Goodman, J. 2013, *PASP*, 125, 306, doi: [10.1086/670067](https://doi.org/10.1086/670067)
- Fu, J.-N., Zhang, C., Marak, K., et al. 2008, *ChJA&A*, 8, 237, doi: [10.1088/1009-9271/8/2/11](https://doi.org/10.1088/1009-9271/8/2/11)
- Fu, J. N., Zha, Q., Zhang, Y. P., et al. 2009, *PASP*, 121, 251, doi: [10.1086/597829](https://doi.org/10.1086/597829)
- Garrido, R., & Rodriguez, E. 1996, *MNRAS*, 281, 696, doi: [10.1093/mnras/281.2.696](https://doi.org/10.1093/mnras/281.2.696)
- Han, Z., Podsiadlowski, P., Maxted, P. F. L., & Marsh, T. R. 2003, *MNRAS*, 341, 669, doi: [10.1046/j.1365-8711.2003.06451.x](https://doi.org/10.1046/j.1365-8711.2003.06451.x)
- Han, Z., Podsiadlowski, P., Maxted, P. F. L., Marsh, T. R., & Ivanova, N. 2002, *MNRAS*, 336, 449, doi: [10.1046/j.1365-8711.2002.05752.x](https://doi.org/10.1046/j.1365-8711.2002.05752.x)
- Henden, A. A., Templeton, M., Terrell, D., et al. 2016, VizieR Online Data Catalog, II/336
- Hintz, E. G., Joner, M. D., Ivanushkina, M., & Pilachowski, C. A. 2004, *PASP*, 116, 543, doi: [10.1086/420858](https://doi.org/10.1086/420858)
- Hübscher, J. 2011, *Information Bulletin on Variable Stars*, 5984, 1
- . 2014, *Information Bulletin on Variable Stars*, 6118, 1
- . 2015, *Information Bulletin on Variable Stars*, 6152, 1
- . 2017, *BAV Journal*, 013, 1
- Hübscher, J., Braune, W., & Lehmann, P. B. 2013, *Information Bulletin on Variable Stars*, 6048, 1
- Hübscher, J., & Lehmann, P. B. 2012, *Information Bulletin on Variable Stars*, 6026, 1
- . 2013, *Information Bulletin on Variable Stars*, 6070, 1
- Hübscher, J., Lehmann, P. B., Monninger, G., Steinbach, H.-M., & Walter, F. 2010, *Information Bulletin on Variable Stars*, 5941, 1
- Iriarte, B. 1952, *ApJ*, 116, 382, doi: [10.1086/145621](https://doi.org/10.1086/145621)
- Irwin, J. B. 1952, *ApJ*, 116, 211, doi: [10.1086/145604](https://doi.org/10.1086/145604)
- Jones, D., & Boffin, H. M. J. 2017, *Nature Astronomy*, 1, 0117, doi: [10.1038/s41550-017-0117](https://doi.org/10.1038/s41550-017-0117)
- Kafka, S. 2020, Observations from the AAVSO International Database. <https://www.aavso.org>
- Kilambi, G. C., & Rahman, A. 1993, *Bulletin of the Astronomical Society of India*, 21, 573
- Lenz, P., & Breger, M. 2005, *Communications in Asteroseismology*, 146, 53, doi: [10.1553/cia146s53](https://doi.org/10.1553/cia146s53)
- Li, L. J., & Qian, S. B. 2010, *AJ*, 139, 2639, doi: [10.1088/0004-6256/139/6/2639](https://doi.org/10.1088/0004-6256/139/6/2639)
- Mahdy, H. A., & Szeidl, B. 1980, *Communications of the Konkoly Observatory Hungary*, 74, 1
- McNamara, D. H. 2011, *AJ*, 142, 110, doi: [10.1088/0004-6256/142/4/110](https://doi.org/10.1088/0004-6256/142/4/110)
- Meylan, G., Burki, G., Rufener, F., et al. 1986, *A&AS*, 64, 25
- Montgomery, M. H., & Odonoghue, D. 1999, *Delta Scuti Star Newsletter*, 13, 28
- Morgenroth, O. 1934, *Astronomische Nachrichten*, 252, 389, doi: [10.1002/asna.19342522402](https://doi.org/10.1002/asna.19342522402)
- Mowlavi, N., Meynet, G., Maeder, A., Schaerer, D., & Charbonnel, C. 1998, *A&A*, 335, 573
- Niu, J.-S., & Li, T. 2018, *PhRvD*, 97, 023015, doi: [10.1103/PhysRevD.97.023015](https://doi.org/10.1103/PhysRevD.97.023015)
- Niu, J.-S., Li, T., Ding, R., et al. 2018, *PhRvD*, 97, 083012, doi: [10.1103/PhysRevD.97.083012](https://doi.org/10.1103/PhysRevD.97.083012)
- Niu, J.-S., Li, T., & Xue, H.-F. 2019, *ApJ*, 873, 77, doi: [10.3847/1538-4357/ab0420](https://doi.org/10.3847/1538-4357/ab0420)
- Niu, J.-S., Fu, J.-N., Li, Y., et al. 2017, *MNRAS*, 467, 3122, doi: [10.1093/mnras/stx125](https://doi.org/10.1093/mnras/stx125)
- Paparo, M., Saad, S. M., Szeidl, B., et al. 1998, *A&A*, 332, 102
- Paxton, B., Bildsten, L., Dotter, A., et al. 2011, *ApJS*, 192, 3, doi: [10.1088/0067-0049/192/1/3](https://doi.org/10.1088/0067-0049/192/1/3)
- Paxton, B., Cantiello, M., Arras, P., et al. 2013, *ApJS*, 208, 4, doi: [10.1088/0067-0049/208/1/4](https://doi.org/10.1088/0067-0049/208/1/4)

- Paxton, B., Marchant, P., Schwab, J., et al. 2015, ApJS, 220, 15, doi: [10.1088/0067-0049/220/1/15](https://doi.org/10.1088/0067-0049/220/1/15)
- Paxton, B., Schwab, J., Bauer, E. B., et al. 2018, ApJS, 234, 34, doi: [10.3847/1538-4365/aaa5a8](https://doi.org/10.3847/1538-4365/aaa5a8)
- Paxton, B., Smolec, R., Schwab, J., et al. 2019, ApJS, 243, 10, doi: [10.3847/1538-4365/ab2241](https://doi.org/10.3847/1538-4365/ab2241)
- Peña, J. H., González, D., & Peniche, R. 1999, A&AS, 138, 11, doi: [10.1051/aas:1999264](https://doi.org/10.1051/aas:1999264)
- Pena, J. H., & Peniche, R. 1986, A&A, 166, 211
- Percy, J. R., Bandara, K., & Cimino, P. 2007, Journal of the American Association of Variable Star Observers (JAAVSO), 35, 343
- Petersen, J. O., & Christensen-Dalsgaard, J. 1996, A&A, 312, 463
- . 1999, A&A, 352, 547
- Pop, A., Turcu, V., & Moldovan, D. 2003, in Astronomical Society of the Pacific Conference Series, Vol. 292, Interplay of Periodic, Cyclic and Stochastic Variability in Selected Areas of the H-R Diagram, ed. C. Sterken, 141
- Poretti, E., Suárez, J. C., Niarchos, P. G., et al. 2005, A&A, 440, 1097, doi: [10.1051/0004-6361:20053463](https://doi.org/10.1051/0004-6361:20053463)
- Quigley, R., & Africano, J. 1979, PASP, 91, 230, doi: [10.1086/130476](https://doi.org/10.1086/130476)
- Rodríguez, E., & Breger, M. 2001, A&A, 366, 178, doi: [10.1051/0004-6361:20000205](https://doi.org/10.1051/0004-6361:20000205)
- Rodríguez, E., & López-González, M. J. 2000, A&A, 359, 597
- Schlafly, E. F., & Finkbeiner, D. P. 2011, The Astrophysical Journal, 737, 103, doi: [10.1088/0004-637x/737/2/103](https://doi.org/10.1088/0004-637x/737/2/103)
- Solano, E., & Fernley, J. 1997, A&AS, 122, 131, doi: [10.1051/aas:1997329](https://doi.org/10.1051/aas:1997329)
- Torres, G. 2010, The Astronomical Journal, 140, 1158, doi: [10.1088/0004-6256/140/5/1158](https://doi.org/10.1088/0004-6256/140/5/1158)
- Townsend, R. H. D., & Teitler, S. A. 2013, MNRAS, 435, 3406, doi: [10.1093/mnras/stt1533](https://doi.org/10.1093/mnras/stt1533)
- Wils, P., Hambsch, F.-J., Lampens, P., et al. 2010, Information Bulletin on Variable Stars, 5928, 1
- Wils, P., Hambsch, F.-J., Robertson, C. W., et al. 2011, Information Bulletin on Variable Stars, 5977, 1
- Wils, P., Panagiotopoulos, K., van Wassenhove, J., et al. 2012, Information Bulletin on Variable Stars, 6015, 1
- Wils, P., Ayiomamitis, A., Vanleenhove, M., et al. 2013, Information Bulletin on Variable Stars, 6049, 1
- Wils, P., Hambsch, F.-J., Vanleenhove, M., et al. 2015, Information Bulletin on Variable Stars, 6150, 1
- Xue, H.-F., Fu, J.-N., Fox-Machado, L., et al. 2018, ApJ, 861, 96, doi: [10.3847/1538-4357/aac9c5](https://doi.org/10.3847/1538-4357/aac9c5)
- Yang, X. H., Fu, J. N., & Zha, Q. 2012, AJ, 144, 92, doi: [10.1088/0004-6256/144/4/92](https://doi.org/10.1088/0004-6256/144/4/92)

APPENDIX

4.1. Calculating X , Y , and Z from [Fe/H]

Following formulas are used to calculate the initial heavy element abundance Z and initial hydrogen abundance X :

$$[\text{Fe}/\text{H}] = \log \frac{Z}{X} - \log \frac{Z_{\odot}}{X_{\odot}}, \quad (3)$$

$$Y = 0.24 + 3Z, \quad (4)$$

$$X + Y + Z = 1, \quad (5)$$

where $X_{\odot} = 0.7381$, $Z_{\odot} = 0.0134$ (Asplund et al. 2009). Equation (4) is provided by Mowlavi et al. (1998). Based on the given values of [Fe/H], we get ($X = 0.756$, $Z = 0.001$), ($X = 0.752$, $Z = 0.002$), and ($X = 0.744$, $Z = 0.004$) as the inputs of the evolutionary models.

4.2. Estimation of the Luminosity

The visual absolute magnitude M_V can be expressed as

$$M_V = V - 5 \log d + 5 - A_V, \quad (6)$$

where $V = 10.264$ mag is taken from AAVSO Photometric All Sky Survey (APASS) catalog (Henden et al. 2016). The distance $d = 404$ pc is provided by Gaia DR2 (Bailer-Jones et al. 2018). The extinction $A_V = 0.363$ mag is obtained from the maps of Schlafly & Finkbeiner (2011).

The absolute bolometric magnitude M_{bol} can be calculated from

$$M_{\text{bol}} = M_V + BC, \quad (7)$$

where the empirical bolometric correction

$$BC = 0.128 \log P + 0.022 \quad (8)$$

for δ Scuti stars is derived by Petersen & Christensen-Dalsgaard (1999).

Then the luminosity can be obtained via $\log L/L_{\odot} = -0.4(M_{\text{bol}} - M_{\text{bol},\odot})$. Here, the bolometric magnitude of the Sun $M_{\text{bol},\odot}$ is taken to be 4.73 mag (Torres 2010). The range of the luminosity is estimated based on the lightness variation of the star, $\Delta V \sim 0.6$ mag. At last, we get the range of the observed luminosity as $\log L/L_{\odot} \in [1.07, 1.31]$.

4.3. Figures and Tables

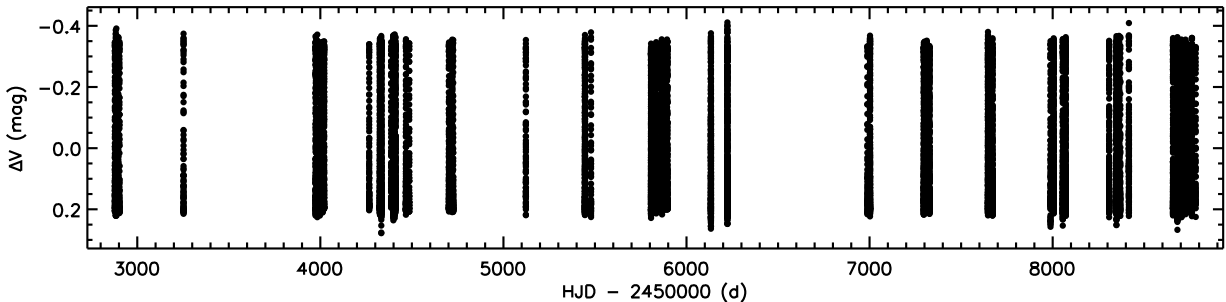


Figure 3. The light curves of DY Peg from 2003 August to 2019 December.

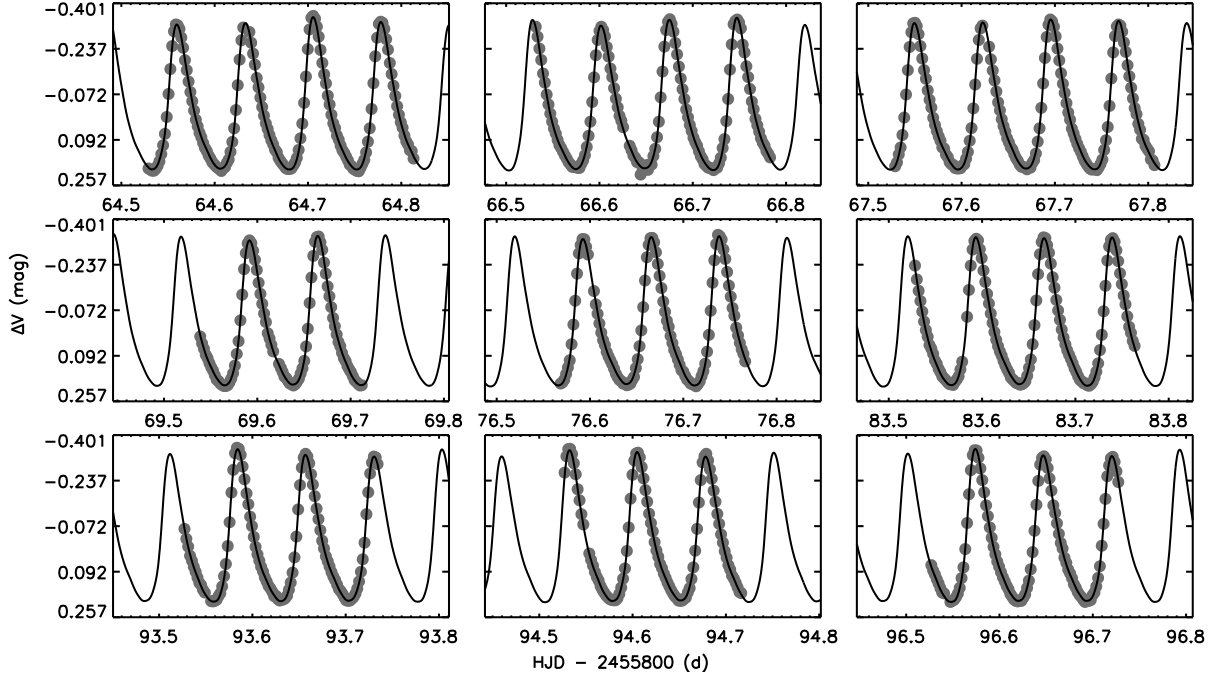


Figure 4. The light curves of DY Peg covering a period of 32 days since 2011 October 30. The solid curves show the fits with the multi-frequency solution.

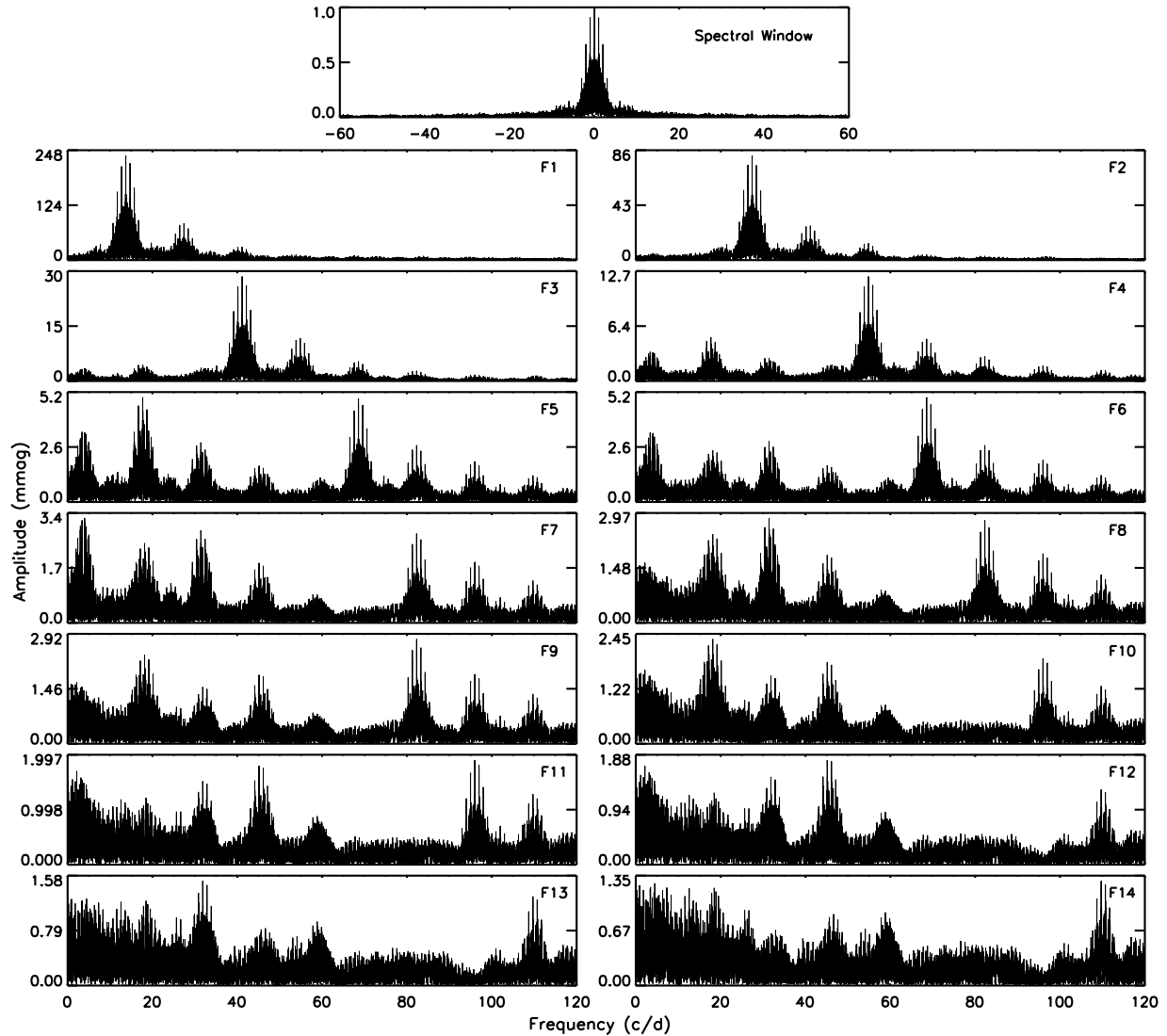


Figure 5. Spectral window and Fourier amplitude spectra of the frequency pre-whitening process for the light curves of DY Peg.

Table 3. Detailed information of the observations for frequency analysis.

Date	Duration (hours)	Number of Observations	σ (mag)
2011 Oct 30	6.7	144	0.001
2011 Nov 1	6.0	127	0.001
2011 Nov 2	6.7	142	0.001
2011 Nov 4	4.2	88	0.001
2011 Nov 11	4.7	100	0.001
2011 Nov 18	5.6	120	0.001
2011 Nov 28	5.0	103	0.001
2011 Nov 29	4.8	94	0.001
2011 Dec 1	4.8	99	0.001

Note: σ denotes the mean error of the observations.

Table 4. Newly determined times of maximum light for DY Peg. Note: asterisks represent the data are not used in $O - C$ analysis.

HJD (2400000+)	σ	HJD (2400000+)	σ	HJD (2400000+)	σ	HJD (2400000+)	σ
52877.72438	0.00004	54406.32897	0.00005	55883.59358	0.00001	57671.66867	0.00002
52877.79792	0.00004	54411.50742	0.00002	55883.66642	0.00001	57671.73953	0.00002
52882.68303	0.00004	54411.57987	0.00002	55883.73958	0.00001	57988.38614	0.00004
52882.75695	0.00004	54467.58710	0.00004	55893.58410	0.00001	58005.59641	0.00002
52884.72583	0.00003	54485.59983	0.00007	55893.65691	0.00001	58005.66960	0.00003
52885.74570	0.00005	54701.82562	0.00004	55894.53214	0.00001	58005.74262	0.00002
52886.69385	0.00003	54702.84695	0.00003	55894.60485	0.00001	58005.81525	0.00002
52886.76697	0.00003	54720.71394	0.00004	55894.67813	0.00002	58005.88827	0.00005
52896.68489	0.00004	54720.78651	0.00004	55896.57398	0.00001	58055.33167	0.00007
52896.75809	0.00004	55122.68311	0.00007	55896.64710	0.00001	58055.40499	0.00007
52902.66618	0.00005	55122.75635	0.00007	56133.43755	0.00003	58071.37567	0.00002
52902.73851	0.00006	55418.51286*	0.00006	56165.3805	0.0001	58071.52164	0.00003
53252.78456	0.00004	55445.38032	0.00002	56223.35532	0.00002	58308.53186	0.00008
53295.21598*	0.00009	55445.45321	0.00002	56223.42830	0.00004	58348.4219	0.0001
53973.73189	0.00003	55445.52690	0.00003	56223.50190	0.00009	58348.49447	0.00007
53975.70061	0.00007	55478.48918	0.00007	56987.69433	0.00002	58362.42380	0.00006
53983.3584	0.0002	55806.51075	0.00001	57002.35206	0.00009	58362.49652	0.00006
53997.65161	0.00006	55834.36863	0.00001	57296.31755	0.00001	58363.44508	0.00006
54003.70445	0.00002	55848.44268	0.00004	57296.38996	0.00002	58369.78916	0.00006
54012.74724	0.00001	55848.51586	0.00005	57296.46383	0.00002	58416.53503	0.00009
54020.69599	0.00002	55864.55996	0.00001	57299.23559	0.00004	58657.55576	0.00004
54020.76879	0.00002	55864.70577	0.00001	57300.40170	0.00005	58657.62869	0.00004
54266.82149	0.00002	55864.77902	0.00003	57300.47481	0.00006	58681.47490	0.00012
54325.74580	0.00006	55866.60212	0.00001	57305.57883	0.00003	58703.42637	0.00007
54325.81846	0.00007	55866.67516	0.00001	57305.65153	0.00004	58703.49882	0.00008
54325.89178	0.00006	55866.74708	0.00004	57312.57982	0.00003	58725.59537	0.00004
54332.67356	0.00006	55867.54975	0.00001	57312.65253	0.00004	58725.66842	0.00002
54332.74681	0.00007	55867.62276	0.00001	57327.31131	0.00004	58725.74119	0.00004
54332.81953	0.00006	55867.69561	0.00001	57646.58186	0.00003	58725.81485	0.00002
54332.89248	0.00008	55867.76839	0.00003	57646.65474	0.00002	58725.88742	0.00003
54386.56584	0.00003	55869.59154	0.00001	57646.72669	0.00002	58748.34909	0.00001
54398.67219	0.00008	55869.66473	0.00001	57646.80075	0.00002	58760.67399	0.00002
54398.74495	0.00007	55876.59286	0.00001	57646.87287	0.00003	58760.74599	0.00002
54398.81767	0.00006	55876.66585	0.00001	57671.52163	0.00003	58781.52988	0.00003
54406.25626	0.00005	55876.73841	0.00002	57671.59525	0.00002		

Table 5. Times of maximum light for DY Peg published in Hübscher et al. (2010, 2013); Hübscher (2011, 2014, 2015, 2017); Hübscher & Lehmann (2012, 2013); Wils et al. (2010, 2011, 2012, 2013, 2015). Note: asterisks represent the data are not used in $O - C$ analysis. Reference: (1) Hübscher et al. (2013); (2) Wils et al. (2010); (3) Hübscher et al. (2010); (4) Wils et al. (2011); (5) Hübscher (2011); (6) Hübscher & Lehmann (2012); (7) Wils et al. (2012); (8) Wils et al. (2013); (9) Hübscher & Lehmann (2013); (10) Hübscher (2014); (11) Hübscher (2015); (12) Wils et al. (2015); (13) Hübscher (2017).

HJD (2400000+)	σ	Ref.	HJD (2400000+)	σ	Ref.	HJD (2400000+)	σ	Ref.
54736.3201	0.0004	(1)	55464.7784	0.0002	(4)	55858.4334	0.0006	(6)
54736.3926	0.0005	(1)	55464.8514	0.0003	(4)	55859.3820	0.0009	(6)
54736.4660	0.0005	(1)	55464.9245	0.0005	(4)	55867.3309	0.0006	(6)
54737.2680	0.0006	(1)	55466.6018	0.0002	(4)	55867.4040	0.0006	(6)
54737.3409	0.0005	(1)	55466.6747	0.0002	(4)	55877.3217	0.0008	(6)
54737.4136	0.0004	(1)	55466.7476	0.0006	(4)	55878.3419	0.0006	(6)
55069.3734	0.0004	(2)	55466.8201	0.0004	(4)	55879.3634	0.0014	(6)
55069.4458	0.0003	(2)	55466.8937	0.0004	(4)	55879.4366	0.0019	(6)
55069.5190	0.0002	(2)	55468.6439	0.0003	(4)	55879.5106	0.0009	(6)
55069.5923	0.0002	(2)	55468.7165	0.0003	(4)	55886.2915	0.0006	(6)
55074.4778	0.0006	(1)	55468.7893	0.0002	(4)	55893.2923	0.0008	(6)
55074.5511	0.0004	(1)	55468.8627	0.0002	(4)	55893.3654	0.0014	(6)
55074.6241	0.0006	(1)	55468.9354	0.0007	(4)	55893.4377	0.0008	(6)
55093.3656	0.0035	(3)	55470.6126	0.0002	(4)	55894.3133	0.0007	(6)
55113.4203	0.0009	(2)	55470.6856	0.0002	(4)	55894.3872	0.0009	(6)
55113.4933	0.0006	(2)	55470.7583	0.0004	(4)	55896.2829	0.0001	(6)
55130.2666	0.0003	(2)	55470.8312	0.0003	(4)	55896.3552	0.0008	(6)
55132.3811	0.0006	(2)	55478.3428	0.0005	(1)	55903.2832	0.0012	(7)
55143.3929	0.0007	(2)	55478.4163	0.0005	(1)	55903.3564	0.0004	(7)
55155.2806	0.0005	(1)	55796.5192	0.0028	(6)	55903.4292	0.0002	(7)
55155.3534	0.0004	(2)	55806.3643	0.0004	(7)	55908.2422	0.0009	(6)
55155.4266	0.0001	(2)	55806.4374	0.0005	(7)	55908.3145	0.0003	(6)
55177.3767	0.0007	(2)	55814.3864	0.0004	(1)	56133.4374	0.0008	(8)
55180.2940	0.0008	(2)	55814.4597	0.0004	(1)	56175.5164	0.0003	(8)
55180.3671	0.0006	(2)	55814.5323	0.0004	(1)	56175.5891	0.0007	(8)
55192.2535	0.0002	(2)	55833.4192	0.0021	(6)	56180.4024	0.0005	(9)
55192.3270	0.0006	(2)	55835.4623	0.0004	(6)	56180.4751	0.0004	(9)
55371.5791	0.0008	(1)	55836.4099	0.0006	(6)	56190.3965	0.0035	(10)
55371.5791	0.0005	(1)	55836.4831	0.0006	(6)	56200.3840	0.0035	(11)
55409.7914	0.0007	(4)	55837.4307	0.0005	(6)	56223.3549	0.0007	(8)
55409.8670	0.0013	(4)	55837.5046	0.0008	(6)	56223.4277	0.0006	(8)
55439.4733	0.0035	(5)	55848.3705	0.0009	(6)	56223.5011	0.0006	(8)

Table 5 continued

Table 5 (*continued*)

HJD	σ	Ref.	HJD	σ	Ref.	HJD	σ	Ref.
(2400000+)			(2400000+)			(2400000+)		
55444.5053	0.0014	(5)	55848.4420	0.0005	(6)	56495.4445	0.0069	(10)
55445.3798	0.0007	(4)	55848.4427	0.0004	(7)	56514.4034	0.0035	(10)
55445.4527	0.0003	(4)	55848.5157	0.0002	(7)	56622.3342	0.0035	(10)
55445.5260	0.0003	(4)	55849.3909	0.0007	(6)	56900.4755	0.0011	(12)
55446.4011	0.0028	(5)	55849.4641	0.0007	(6)	56900.5479	0.0004	(12)
55451.5064	0.0028	(5)	55849.5366	0.0008	(6)	56900.6210	0.0003	(12)
55453.3285	0.0035	(5)	55852.4536	0.0004	(1)	56981.3496	0.0035	(11)
55459.6009	0.001	(4)	55854.2768	0.0003	(7)	56981.4225	0.0035	(11)
55459.6738	0.0004	(4)	55854.3501	0.0002	(7)	57002.3529	0.0004	(12)
55459.7464	0.0002	(4)	55856.3923	0.0004	(6)	57296.3070*	0.0004	(13)
55459.8196	0.0003	(4)	55856.4648	0.0005	(6)	57296.3799*	0.0004	(13)
55459.8924	0.0006	(4)	55857.3400	0.0006	(6)	57296.4531*	0.0005	(13)
55464.6327	0.0002	(4)	55857.4130	0.001	(6)	57296.5260*	0.0004	(13)
55464.7053	0.0003	(4)	55857.4853	0.0007	(6)	57296.5984*	0.0005	(13)

Table 6. The observed stellar parameters of DY Peg.

Parameter	Value	Reference
[Fe/H] (dex)	-0.8 ± 0.2	Burki & Meylan (1986)
	-0.56	Peña et al. (1999)
	-0.8	Hintz et al. (2004)
T_{eff} (K)	[6750, 7950]	Burki & Meylan (1986)
	[6910, 8270]	Peña et al. (1999)
	[7330, 8230]	Hintz et al. (2004)
	[7200, 8350]	Kilambi & Rahman (1993)
$v \sin i$ (km s ⁻¹)	23.6	Solano & Fernley (1997)

Table 7. Best-fit seismic models and the corresponding parameters.

Z	v_{eq} (km s ⁻¹)	M (M _⊕)	T_{eff} (K)	$\log L/L_{\odot}$	f_0 (c days ⁻¹)	f_1 (c days ⁻¹)	f_2 (c days ⁻¹)	f_0/f_1	$(1/P_0)(dP_0/dt)$ (yr ⁻¹)
0.001	23.6	0.93	6535	0.65	13.71241	17.7099	18.166	0.7743	1.1×10^{-9}
0.001	150	0.92	6421	0.61	13.71193	17.7305	18.373	0.7734	8.8×10^{-10}
0.002	23.6	1.02	6602	0.70	13.71301	17.6838	18.079	0.7754	9.7×10^{-10}
0.002	150	1.00	6455	0.65	13.71291	17.6864	18.222	0.7753	7.5×10^{-10}
0.004	23.6	1.20	6931	0.85	13.71327	17.6964	18.105	0.7749	9.7×10^{-10}
0.004	150	1.10	6461	0.68	13.71246	17.6869	18.130	0.7753	5.8×10^{-10}